ELSEVIER

Journal of Hazardous Materials B97 (2003) 315–327

Journal of Hazardous Materials

www.elsevier.com/locate/jhazmat

Oil mobility in a saturated water-wetted bed of glass beads

Francesco Gioia*, Guido Alfani, Sergio Andreutti, Fabio Murena

Dipartimento di Ingegneria Chimica, Università di Napoli Federico II, Piazzale Tecchio, 80122 Napoli, Italy

Received 5 May 2002; accepted 7 October 2002

Abstract

The mobilization of an oil bank in a packed bed of glass beads saturated with an aqueous phase has been studied both theoretically and experimentally. The size of the glass beads was varied in the range between 0.5 and 5 mm. Two oils (hexadecane and hexane) with viscosities different for an order of magnitude and densities smaller than that of water have been used. A few more runs have been carried out using perchloroethylene (PCE), with density greater than that of water. The interfacial tension in the aqueous phase was varied in a quite large range (0.38–39.1 dyn/cm) by adding surfactants to the water. The glass assembly made it possible to follow the evolution of the dyed oily phase by the use of a digital camera. A very simple stochastic model for describing the porous structure of the packed bed made it possible to set a criterion for determining the probability of mobilization of ganglia which are produced by the fragmentation of the oil bank. The same model permits also to estimate the probability function of the velocity of a ganglion of an assigned size.

Keywords: NAPL mobility in aquifer; Oil ganglia velocity; Interfacial tension; Enhanced NAPL mobility

1. Introduction

The flow through water-saturated granular porous media of a dispersed immiscible phase is of great practical interest in connection with underground-water pollution by organic solvents and other petroleum derived products, which may enter the subsurface. When a bank of an oily phase is spilled in a water-saturated unconsolidated granular porous medium, the fragmentation of this phase in ganglia and/or droplets is the most remarkable phenomenology observed. These fragments may remain entrapped in the porosity or move through the porous medium even though slowly. The phenomenon of the fragmentation has

Abbreviations: PCE, perchloroethylene (tetrachloroethylene)

* Corresponding author. Tel.: +39-81-7682277; fax: +39-81-2391800.
E-mail address: gioia@unina.it (F. Gioia).

0304-3894/02/$ – see front matter
PII: S0304-3894(02)00281-9

Nomenclature

Abs	absolute value
Bo	Bond number (see Eq. (2))
Ca	capillary number (see Eq. (8))
D_p	diameter of a glass bead (cm)
k	intrinsic permeability of the porous bed (see Eq. (1); cm^2)
k_{ro}	relative permeability to the oily phase
k_{rw}	relative permeability to the aqueous phase
$\hat{\boldsymbol{k}}$	unit vector in the z-direction (upward)
Δl	characteristic size of the ganglion (cm)
r_b	radius of the oil ganglion (cm)
r_n	radius of the pore neck (cm)
r_p	radius of the pore, $r_p \approx D_p/2$ (cm)
$\boldsymbol{v}_o$	velocity of the ganglion (cm/s)
$v_{o,m}$	measured velocity of a ganglion (cm/s)
$v_{o,max}$	maximum velocity due to buoyancy force only (cm/s)
$\boldsymbol{v}_w$	Darcy's velocity of the aqueous phase (cm/s)
V_o	volume of the oil ganglion (cm^3)
$\cdot$	scalar product

Greek letters

ε	porosity
μ_m	"combination viscosity", $\mu_m = f\bar{\mu}_m$ (see Eqs. (21) and (23); (g/(cm s)))
μ_o	viscosity of the oil (g/(cm s))
μ_w	viscosity of the aqueous phase (g/(cm s))
$\Delta\rho$	is $\rho_w - \rho_o$ (g/cm^3)
ρ_o	density of the oil (g/cm^3)
ρ_w	density of the aqueous phase (g/cm^3)
σ_{ow}	interfacial tension between the oil and the aqueous phase (dyn/cm)

a great importance on the rate of contamination of the water phase. In fact, the specific interface area increases noticeably with respect to that of the oil bank, thus increasing the rate of solubilization of the contaminant.

Many papers, with quite different approaches to the study of this multifaceted problem, have been published. Ng and Payatakes [1], Payatakes et al. [2], Dias and Payatakes [3], aim at obtaining a macroscopic description of the mobilization and break up phenomenology focusing the attention on the microscopic mechanism of the two-phase flow. They set an idealized model of the geometrical structure of unconsolidated packings for describing the local topology of the porous medium. Then, assigned the initial size, shape and orientation of a ganglion, they provide a complex stochastic simulation of its motion and break up. Avraam and Payatakes [4], following the same approach, use for their accurate experiments a model porous medium, specifically constructed, with a pore network based on a square lattice. Other Authors [5,6] focus the attention on the characterization of the ganglia

size distribution in unconsolidated porous media, as a function of the particle size. The sizes of the ganglia formed by immiscible liquids are experimentally evaluated infusing liquid styrene in the porous medium (sand or glass beads) saturated with water. Then the styrene is solidified by polymerisation. The removal of the porous medium produces solid ganglia, which can be analyzed for determining their size distribution. An alternative approach for measuring ganglia [7] is to infuse a transparent porous medium with a dyed organic liquid, to photograph the ganglia, and to determine the size distribution by image analysis. Pennel et al. [8], in order to investigate on the mobilization of a dispersed phase during surfactant flushing, perform column experiments in unconsolidated porous media (Ottawa sand). They set a theoretical useful criterion for predicting the mobilization conditions of the dispersed phase. The present paper follows this last approach in attempting to set, from macroscopic observations and theoretical considerations, a criterion for determining the mobilization conditions of a dispersed phase, and the velocity of ganglia in unconsolidated water-saturated porous media. In order to reduce the overall complexity of the problem, the study has been carried out reducing to the minimum the uncertainties related to the local geometry of the porous structure. To this purpose, the experiments have been performed in a glass column filled with uniformly sized spherical glass beads. This feature allowed us to set up a very simple stochastic model for determining the mobilization criterion as function of the prevailing physical parameters and variables. The transparency of the experimental set up was of a great help for observing the phenomenology of mobilization and fragmentation, and for comparing the observations with the theoretical results. The experiments were carried out using bead diameters in the range 0.5–5 mm and interfacial tensions of the aqueous phase in a quite large range (0.38–39.1 dyn/cm).

2. Experimental part

2.1. Apparatus and materials

The experiments were carried out in a glass column (4 cm diameter, 50 cm height). Runs with glass beads of different size, different oils (hexadecane and hexane, lighter than water, and perchloroethylene (PCE), heavier than water), and aqueous phases having different interfacial tension (by adding surfactants to water) were accomplished. The column was filled with glass beads and saturated with the aqueous phase. The oil (hexadecane and hexane) was injected by a syringe through an injection port at the bottom of the column (for the case of PCE, the oil was injected at the top of the column). Preliminarily, in a different column in which it was possible to have a water flow through the bed of glass beads and equipped to measure pressure drops (by means of a differential reverse U-Tube manometer containing water) as a function of the liquid flow rate, it was measured the intrinsic permeability of the packed bed. The experiments showed that the pressure drop through the bed was well described by the Ergun equation [9]. Therefore, the intrinsic permeability was calculated by this equation as

$$k = \frac{D_p^2}{150} \frac{\varepsilon^3}{(1-\varepsilon)^2} \tag{1}$$

Table 1
Porous media properties

D_p (mm)	ε	k (cm^2)
0.5	0.38	2.4×10^{-6}
1	0.39	1.1×10^{-5}
2	0.41	5.3×10^{-5}
3	0.42	1.3×10^{-4}
5	0.43	4.1×10^{-4}

The porosity of the bed was determined as follows: the beads were loaded in a graduate cylinder (same diameter as the column) and their apparent volume V_a was recorded. The bed was then saturated with water whose volume V_w was recorded too. By definition it is $\varepsilon = V_w/V_a$.

The oil/aqueous phase interfacial tension was varied using two different surfactants: Tween 80 (polioxyethylen-sorbitan-monooleate) and DSS (dyoctyl-sulfosuccinate-sodium salt). It was measured by an Optical Contact Angle Meter tensiometer (CAM 200, KSV Instruments Ltd.). The oil, was red colored by adding about 1 wt.% of a die immiscible with water. The addition of the die did not alter significantly the oil/water interfacial tension. The evolution of the oil through the column was followed shooting pictures at different times by a digital camera.

Preliminary replicates were run by adopting different methods for introducing the oil at the bottom of the bed: by a syringe, injecting slowly (5 ml of oil in 15 min) or quickly; by putting the oil at the bottom of the empty column, adding the beads and last introducing the water phase. The evolution of the oil did not show significant differences on the three different loading techniques. Therefore, the majority of runs was done by injecting (slowly) the oil by the syringe. The details of the operating conditions of the experiments are reported in Tables 1 and 2. Notice that for $D_p = 0.5$ mm the permeability reported in Table 1 checks with typical values directly measured in aquifers; larger D_p simulate sands.The experiments were carried out with stagnant aqueous phase, in order to study the influence of buoyancy

Table 2
Fluids properties

Run	Oil	Aqueous phase	μ_w (cP)	$\Delta\rho$ (g/ml)	σ_{ow} (dyn/cm)
6, 7	Hed	W	1.0	0.226	38.8
1, 3	Hed	W + Tw (4 wt.%)	1.2	0.226	7.4–8.4
8, 18	Hed	W + DSS (1 wt.%)	3.5	0.226	0.43
5, 11, 15, 19	Hex	W	1.0	0.341	38.7–39.1
2, 4, 24, 26	Hex	W + Tw (4 wt.%)	1.2	0.341	10.0–11.3
9, 16, 17, 22, 27	Hex	W + DSS (1 wt.%)	3.5	0.341	0.38–0.49
23	PCE	W	1.0	−0.62	36.5
25, 28	PCE	W + Tw (4 wt.%)	1.2	−0.62	9.8

Hed, *n*-hexadecane; W, water; Tw, surfactant Tween 80; DSS, surfactant DSS; hex, *n*-hexane; PCE, perchloroethylene (tetrachloroethylene); $\mu_{Hed} = 2.89$ cP; $\mu_{Hex} = 0.29$ cP; $\mu_{PCE} = 0.85$ cP at $T = 25\,^{\circ}$C.

forces on the mobilization of the oily phase. In such conditions the phenomenology depends only on the value of the Bond number, defined as

$$Bo = \frac{kk_{\mathrm{rw}}\,\Delta\rho g}{\sigma_{\mathrm{ow}}} \tag{2}$$

It must be pointed out that the Bond number assumes positive or negative values depending on the value of $\Delta\rho$. The relative permeability to the water phase k_{rw} tends to unity as the saturation tends to zero. In our experiments the oil ganglia are largely dispersed in the column; therefore we set $k_{\mathrm{rw}} = 1$. More details on the experimental procedure are reported in [10].

2.2. Experimental results

Sharply different phenomenologies are observed upon the injection of the oily phase (hexane and hexadecane) at the bottom of the porous bed filled with the stagnant aqueous phase. They are depending on the value of the Bond number. The experiments confirmed what was already known, that the rising of the oil does not occur as a continuous phase. Rather breakup and stranding of oil ganglia occur during the motion. A bank of oil for which the *Bo* is below the critical value (i.e. 10^{-3}), upon injection shows an initial mobility due to fingers that move along preferential patterns. Eventually, these fingers break up in smaller ganglia and/or droplets (with a size comparable to that of the particles), which remain immobile in the interstices of the porous bed. For values of $Bo > 10^{-2}$ the ganglia generated from the bank definitely move, undergoing stranding and successive fragmentation, "dynamic break-up", until all the oil injected reaches the top of the column. It must be remarked that even the smaller droplets, in their majority, reach the top of the column. For $10^{-3} < Bo < 10^{-2}$, an intermediate situation is observed (partial mobility). For this case only the large ganglia move and undergo fragmentation, generating smaller ganglia entrapped in the porous medium. For the case of PCE ($\Delta\rho < 0$, then $Bo < 0$) a similar phenomenology, but in the opposite direction, has been observed.

The experimental results described above are summarized in Fig. 1.

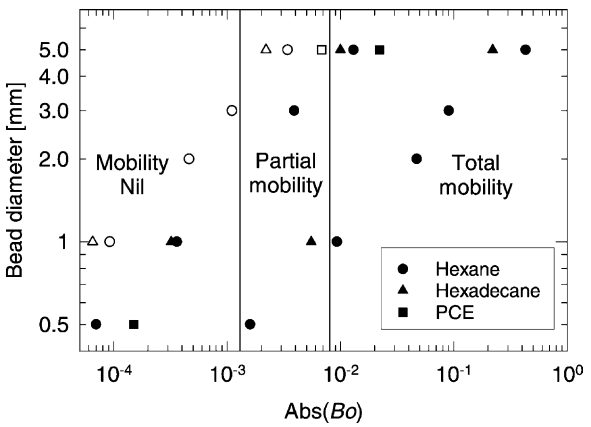

Fig. 1. Experimental mobility diagram. Empty symbols are for pure water, filled are for water with surfactant.

As expected, the oil mobility significantly decreases with decreasing particle size, i.e. hexane in contact with water is partially mobile in a bed of 5 mm beads, and is totally immobile in a bed of 1 mm beads ($9.5 \times 10^{-5} \leq Bo \leq 3.5 \times 10^{-3}$).

Oil mobility strongly increases with decreasing interfacial tension, i.e. for the case of a 3 mm porous medium, hexane is immobile when in contact with water ($\sigma_{ow} = 39.1$ dyn/cm), is partially mobile when in contact with a Tween 80 aqueous solution ($\sigma_{ow} = 11.3$ dyn/cm), is totally mobile when in contact with a DSS aqueous solution ($\sigma_{ow} = 0.49$ dyn/cm).

Dynamic viscosity does not influence the mobilization (for the range of values investigated). In fact both hexane and hexadecane show the same mobility in experiments run at the same conditions (same bead diameter and aqueous phase, then similar Bond number), even though dynamic viscosity differs for an order of magnitude.

3. Modeling

The forces acting on an oil globule entrapped in a pore of a saturated water-wetted porous medium are clearly described by Pennel et al. [8]. Two kinds of forces act on the globule: a driving force $\boldsymbol{F}_{dr}$, which tends to mobilize it, and the capillary retention force $\boldsymbol{F}_{c}$, which is opposite to $\boldsymbol{F}_{dr}$. The former is due to the pressure gradient in the water phase and to the weight of the globule. The latter is related to the work required for deforming the surface of the globule, which, for getting off the pore, must thread its way through a pore neck with a radius smaller than that of the pore.

Considering a motion, on the overall vertical, in the porous medium, and setting a z-axis directed vertically upward it is

$$\boldsymbol{F}_{dr} = \left(-\frac{\partial P_w}{\partial z} - \rho_o g \right) V_o \hat{\boldsymbol{k}} \tag{3}$$

where $\hat{\boldsymbol{k}}$ is the unit vector in the z-direction. V_o is the ganglion volume, which may be approximated as $\pi r_b^2 \, \Delta l$ (πr_b^2 is the cross-sectional area of the ganglion and Δl is its length).

According to Pennel et al. [8], the magnitude of the retention capillary force may be obtained from Laplace's equation as

$$|\boldsymbol{F}_c| = \frac{2\beta\sigma_{ow}}{r_n} \pi {r_b}^2 \tag{4}$$

where the geometric factor β is defined as

$$\beta = 1 - \frac{r_n}{r_p} \tag{5}$$

We assume that the largest value of r_p is equal to the radius of the glass bead and that the radius of the pore neck r_n may range between 0 and r_p. The value zero refers to pores surrounded by beads which touch one another all around the pore (the pore is occluded). Values of r_n larger than r_p are not considered inasmuch as they represent unstable situations: beads could fall in the pore. Therefore, β assumes values in the range [0, 1].

Notice that it must be $\boldsymbol{F}_{\mathrm{dr}} \cdot \boldsymbol{F}_{\mathrm{c}} < 0$ as $\boldsymbol{F}_{\mathrm{c}}$ is always opposed to $\boldsymbol{F}_{\mathrm{dr}}$. The z component of the pressure gradient may be obtained from the Darcy's law:

$$\boldsymbol{v}_{\mathrm{w}} = -\frac{k}{\mu_{\mathrm{w}}}\left(\frac{\partial P_{\mathrm{w}}}{\partial z} + \rho_{\mathrm{w}} g\right)\hat{\boldsymbol{k}} \tag{6}$$

Combining Eqs. (3), (4) and (6), we write the following Eq. (7), which gives the mobility condition of an oil ganglion in a saturated porous bed:

$$\left|\left(\frac{\mu_{\mathrm{w}}\boldsymbol{v}_{\mathrm{w}}}{k} + \Delta\rho\, g\hat{\boldsymbol{k}}\right) V_{\mathrm{o}}\right| > \frac{2\beta\sigma_{\mathrm{ow}}}{r_{\mathrm{n}}}\pi r_{\mathrm{b}}^2 \tag{7}$$

Eq. (7) expresses the condition that the driving force for the motion $\boldsymbol{F}_{\mathrm{dr}}$ on the oil globule is larger than the capillary retention force $\boldsymbol{F}_{\mathrm{c}}$. Introducing the Bond number (see Eq. (2)) and the capillary number:

$$\mathrm{Ca} = \frac{\mu_{\mathrm{w}}\boldsymbol{v}_{\mathrm{w}}}{\sigma_{\mathrm{ow}}} \cdot \hat{\boldsymbol{k}} \tag{8}$$

Eq. (7) becomes

$$|\mathrm{Ca} + Bo| > \frac{2\beta k}{r_{\mathrm{n}}\,\Delta l} \tag{9}$$

When condition (9) is verified the ganglion moves: upward if $\mathrm{Ca} + Bo > 0$; downward if $\mathrm{Ca} + Bo < 0$.

It must be pointed out that Eq. (9) is the straightforward extension to a porous bed of the mobilization condition which is strictly valid for a single globule of oil in a geometrically well defined pore [8]. In fact, the geometric factor β/r_{n} is deterministically related to the geometry of the pore assembly. As a matter of fact even in a packed bed filled with uniformly shaped and sized glass beads, the value of geometric factor β/r_{n} changes casually in the bed. Therefore, a stochastic approach seems more appropriate for describing the overall motion of oil ganglia in the bed. Consider the ratio $a = r_{\mathrm{n}}/r_{\mathrm{p}}$. Having assumed that the radius of the pore neck r_{n} may range between 0 and r_{p}, the ratio a has values in the range [0, 1]. Therefore, we assume that the dimensionless variable a has a probability distribution given by the normal density function PDF(a), with mean = 0.5 and variance = 0.125. With this choice, it is practically excluded that a has values outside the range [0, 1], i.e. $a \in [0, 1]$. Then, the geometric factor β/r_{n} stochastically defined becomes

$$\frac{\beta}{r_{\mathrm{n}}} = \frac{b}{r_{\mathrm{p}}} \tag{10}$$

where

$$b = \frac{1-a}{a} \tag{11}$$

Having assigned PDF(a), it results set the density function PDF(b) of b ($b \in [0, \infty]$), which may be obtained from that of a by a change of variable. In the following we will use the stochastic parameter b/r_{p} in place of β/r_{n}. Once the porous structure of the bed has been characterized by the stochastic parameter b, it is possible to develop a quantitative analysis

of the mobilization of oil ganglia. For brevity we will specifically refer to the following experimental conditions: oil lighter than the saturation aqueous phase, which is kept stagnant ($\Delta\rho > 0$ then $Bo > 0$; Ca $= 0$). For this case $\boldsymbol{F}_{\mathrm{dr}}$ is the buoyancy force directed upward, while $\boldsymbol{F}_{\mathrm{c}}$ is directed downward. Then the mobility condition Eq. (9) for the ganglion of size Δl may be written as

$$b < \frac{\Delta l\, r_{\mathrm{p}}}{2k} Bo \tag{12}$$

The probability that the ganglion mobilizes is

$$m = \int_0^{b_{\mathrm{cr}}} \mathrm{PDF}(b)\, \mathrm{d}b \tag{13}$$

where

$$b_{\mathrm{cr}} = \frac{\Delta l\, r_{\mathrm{p}}}{2k} Bo = \frac{\Delta l\, r_{\mathrm{p}}\, \Delta\rho\, g}{2\sigma_{\mathrm{ow}}} \tag{14}$$

Namely, m is the probability that the variable b is not larger than its critical value b_{cr}. Therefore, we are led to the conclusion that essentially $m = m(Bo, D_{\mathrm{p}}, \Delta l)$. A more detailed description of the dependence of m on the structure of the porous material and on the properties of the fluids may be obtained by inspection of Eq. (14). In particular, the mobilization probability increases with the size of the ganglion and with the size of the particles, but decreases as the interfacial tension increases. Graphs of the mobilization probability versus Bo, for three ganglion sizes in a bed of 5 mm glass beads, are shown, as an example, in Fig. 2.

It is worth to point out that the fact that smaller ganglia are less mobile is physically consistent. In fact, the driving force for mobilization is proportional to the volume of the ganglion, while the retention force, which opposes the movement, is proportional to its surface area. Therefore, the ratio $F_{\mathrm{c}}/F_{\mathrm{dr}}$ increases as the size of the ganglion decreases making the retention force predominant.

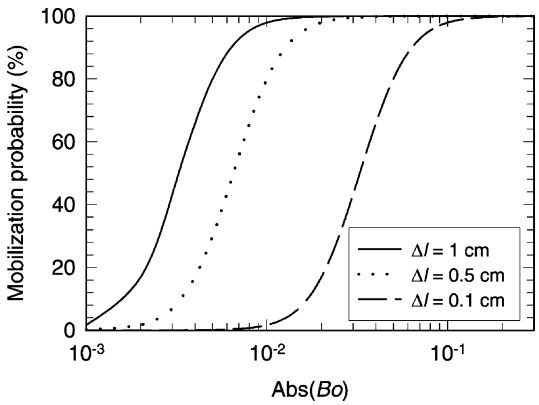

Fig. 2. Mobilization probability vs. Bond number. Curves are referred to glass beads of diameter $D_{\mathrm{p}} = 5$ mm.

Table 3
Comparison between observed and model mobility of oil ganglia for $D_p = 5$ mm

Run	*Bo*	Observed ganglia, Δl (cm)	Observed[a] mobility	Model mobility, *m* (%; Eq. (13))
6	2.3×10^{-3}	1	Partial	24.4
		0.5	Nil	2.8
5	3.5×10^{-3}	1	Partial	55.6
		0.5	Nil	11.4
3	1.1×10^{-2}	0.5	Total	84.6
4	1.3×10^{-2}	0.5	Total	90.8
18	2.1×10^{-1}	0.1	Total	99.8
17	3.6×10^{-1}	0.1	Total	100
23	-6.8×10^{-3}	0.5	Partial	53.3

[a] From Fig. 1.

3.1. Comparison with experimental results

Some typical ganglion sizes and their mobility conditions (nil, partial, total) are recorded from the pictures taken during each experiment. Then the percent mobility is calculated, for such ganglia, by Eq. (13). The result of this analysis is reported in Table 3, which for brevity refers to 5 mm glass beads only. Inspection of this table shows that the mobility calculated by the model equation, as compared with the observations of Fig. 1, gives the following correlation: an observed total mobility corresponds to a model mobility ranging between 84.6 and 100%. A mobility nil corresponds to model values in the range 2.8–11.4%. The visual observations of Fig. 1 are, for their nature, uncertain. Therefore, it is not possible to set model values for which the transitions nil/partial and partial/total take place. Only ranges may be established, i.e. nil/partial in the range 11.4–24.4% of model mobility and partial/total in the range 55.6–84.6%. Similar results are obtained for particle diameters 1 and 2 mm.

For determining the mobility of a bank of oil one checks first the value of the Bond number. If *Bo* is above 10^{-2} the bank is totally mobile. If *Bo* is below 10^{-3} the bank mobility is nil. For *Bo* in the range 10^{-3} to 10^{-2} one checks (by Eq. (13)) the probability of mobilization *m* of the smallest droplets ($\Delta l = D_p$), which have the minimum tendency to move. For example if we consider run 5, larger ganglia ($\Delta l = 1$ cm) show a partial mobility and have a probability of mobilization $m = 55.6\%$, smaller ones ($\Delta l = 0.5$ cm) are stranded in the porous medium and have a probability of mobilization $m = 11.4\%$.

3.2. Velocity of oil ganglia

We assume that the Darcy's law, which is strictly valid for the motion of a continuos phase, may be extended to the motion of the disconnected oil ganglia in the porous bed. As a matter of fact, this is somewhat a strong assumption which could be reasonably accepted in the case that $\Delta l \gg D_p$. In vector notation it is

$$\boldsymbol{v}_o = -\frac{k}{\mu_m}\left(\frac{\partial P_o}{\partial z} + \rho_o g\right)\hat{\boldsymbol{k}} \tag{15}$$

where $\boldsymbol{v}_o$ is the velocity of the oil ganglia; $(\partial P_o)/(\partial z)\hat{\boldsymbol{k}}$ is the z component of the pressure gradient in the oil ganglion and μ_m is a combination of the viscosities of the two phases. The relative permeability k_{ro} to the oily phase is not included in Eq. (15). In fact, the use of the combination viscosity μ_m takes into account the oil/water relative permeability. The pressure in the oil phase is the sum of the pressure in the water phase and of the capillary pressure, i.e. $P_o = P_w + P_c$. Therefore,

$$\frac{\partial P_o}{\partial z}\hat{\boldsymbol{k}} = \left(\frac{\partial P_w}{\partial z} + \frac{\Delta P_c}{\Delta l}\right)\hat{\boldsymbol{k}} \tag{16}$$

where it has been set as

$$\frac{\partial P_c}{\partial z} \cong \frac{\Delta P_c}{\Delta l} \tag{17}$$

Using Eqs. (4)–(6) and (16), Eq. (15) may be rearranged to give

$$\boldsymbol{v}_o = \frac{\sigma_{ow}}{\mu_m}\left(\mathrm{Ca} + Bo \pm \frac{2bk}{r_p\,\Delta l}\right)\hat{\boldsymbol{k}} \tag{18}$$

The sign is chosen considering that the capillary retention force is always opposite to the driving force. Notice that $\boldsymbol{v}_o$ points in the direction of the driving force, i.e. $\boldsymbol{v}_o \cdot \boldsymbol{F}_{dr} > 0$. Hence, it must be set $\boldsymbol{v}_o = 0$ whenever the whole term in the brackets has a sign opposite to that of $(\mathrm{Ca} + Bo)$. In conclusion,

$$\textit{if } |\mathrm{Ca} + Bo| > \frac{2bk}{r_p\,\Delta l}, \quad \text{then } (\boldsymbol{v}_o \cdot \hat{\boldsymbol{k}}) = \mathrm{sign}(\mathrm{Ca} + Bo)\frac{\sigma_{ow}}{\mu_m}\left(|\mathrm{Ca} + Bo| - \frac{2bk}{r_p\,\Delta l}\right) \tag{19}$$

The probability density function $\mathrm{PDF}(\boldsymbol{v}_o)$ and, hence, the probability $\mathrm{PF}(v_o)$ of $|\boldsymbol{v}_o|$, for an assigned ganglion size Δl, can be calculated by a change of variable in the density function of b.

The maximum value of v_o is obtained setting zero the capillary retention force, i.e. $b = 0$. Namely, for $\mathrm{Ca} = 0$ it is

$$v_{o,\max} = \frac{k\,\Delta\rho g}{\mu_m} \tag{20}$$

3.3. Combination viscosity μ_m

The viscosity μ_m which appears in Eq. (18) is a combination of the viscosity of the two fluids, i.e. $\mu_m = f(\mu_o, \mu_w)$. It is reported by Clift et al. [11] that when a liquid moves as a dispersed-phase (e.g. droplets) in an immiscible liquid (continuous phase), the velocity of the dispersed-phase (droplets) may be described using a "combination viscosity" that is

$$\bar{\mu}_m = \frac{(2/3) + (\mu_o/\mu_w)}{1 + (\mu_o/\mu_w)} \cdot \mu_w \tag{21}$$

where μ_w is the viscosity of the continuous phase. Unfortunately, no information is reported in the literature on a possible expression of μ_m for the case of a dispersed fluid moving in a porous medium. Therefore, the best we can do is to assume that $\mu_m = f\bar{\mu}_m$ and determine

Table 4
Calculation of the parameter f for $D_p = 5\,mm$

Oil	Aqueous phase	*Bo*	Observed ganglia, Δl (cm)	Observed velocity, $v_{o,m}$ (cm/s)	Model velocity $(\bar{v}_o)_{f=1}$ (cm/s)	Parameter f	Combination viscosity, μ_m for $f = 3$ (cP)
Hed	W	2.3×10^{-3}	1	0.3	0.64	2.1	2.7
Hex	W	3.5×10^{-3}	1	1	3.4	3.4	2.2
Hed	W + Tw (4 wt.%)	1.1×10^{-2}	0.5	1.2	3.1	2.6	3.2
Hex	W + Tw (4 wt.%)	1.3×10^{-2}	0.5	2.3	7.1	3.1	2.6
Hed	W + DSS (1 wt.%)	2.1×10^{-1}	0.1	1.1	2.6	2.4	8.6
Hex	W + DSS (1 wt.%)	3.6×10^{-1}	0.1	1.8	5.0	2.8	7.3
PCE	W	-6.8×10^{-3}	0.5	1.9	5.1	2.7	2.5

Hed, *n*-hexadecane; W, water; Tw, surfactant Tween 80; DSS, surfactant DSS; hex, *n*-hexane; PCE, perchloroethylene (tetrachloroethylene); $\mu_{Hed} = 2.89\,cP$; $\mu_{Hex} = 0.29\,cP$; $\mu_{PCE} = 0.85\,cP$ at $T = 25\,^{\circ}C$; $\mu_w = 1\,cP$; $\mu_{w+Tw} = 1.2\,cP$; $\mu_{w+DSS} = 3.5\,cP$ at $T = 25\,^{\circ}C$.

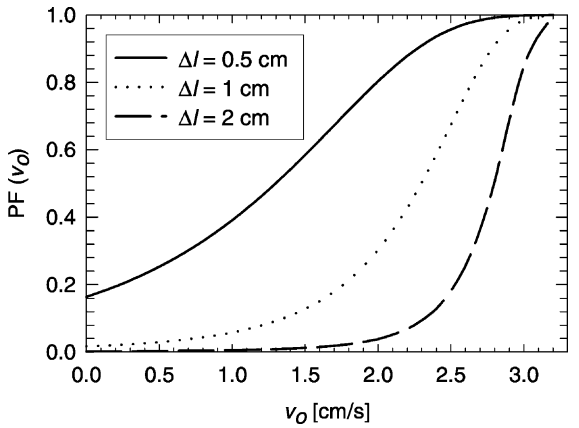

Fig. 3. Probability function of the velocity of oil ganglia for ganglia of different size. Curves are referred to: hexadecane/aqueous solution Tween 80 ($\sigma_{ow} = 8.4$ dyn/cm); $D_p = 5$ mm, $k = 4.1 \times 10^{-4}$ cm^2; $Bo = 1.1 \times 10^{-2}$.

experimentally the adjustable parameter *f*. The procedure is as follows: the velocity ($v_{o,m}$) of a number of ganglia of different sizes of the oils was measured; then the expected value of v_o for $f = 1$ was calculated by the equation

$$(\bar{v}_o)_{f=1} = \int_0^{v_{o,max}} v_o \, \mathrm{PDF}(v_o) \, \mathrm{d}v_o \tag{22}$$

The parameter *f* was determined as

$$f = \frac{(\bar{v}_o)_{f=1}}{v_{o,m}} \tag{23}$$

This procedure yields values of *f* lying in a narrow range [2.1, 3.4] for all fluids used in our experiments, even though both μ_o and μ_w have a much larger variation. An example of such calculation is given in Table 4.

The curves of Fig. 3 are drawn for $f = 3$. It must be remarked that *f* is an adjustable parameter and the value determined applies to the regularly shaped and sized particles used in our experiments. Fig. 3 shows, consistently with the previous results on mobilization, that ganglia of larger size have smaller probability of zero velocity and tend to assume a larger velocity.

4. Conclusions

The experimental results and a simple stochastic model permit to determine the mobility condition of a bank of oil infused in an unconsolidated porous material, saturated with an aqueous phase. First one checks if $|Bo|$ is well above 10^{-2}. In this case, the bank will undergo a "dynamic break-up" generating ganglia which go through stranding and successive fragmentation and will move toward the top (if $Bo > 0$) until all the oil has left the porous

bed. Even the smaller droplets, in their majority, reach the top of the column. If $|Bo| < 10^{-3}$ the bank will show an initial mobility due to fingers that move along preferential patterns. Eventually these fingers break up in smaller ganglia and/or droplets (with a size comparable to that of the particles), which will remain entrapped in the interstices of the porous bed. For $10^{-3} < |Bo| < 10^{-2}$ a partial mobility is predicted. Only part of the oil (the larger ganglia) will move and eventually undergo fragmentation, generating smaller ganglia entrapped in the porous bed. For this case, the stochastic model is useful for determining whether ganglia of an assigned size will move or remain entrapped in the porous medium. Thus, permitting to determine the smallest size of ganglia that may leave the bed.

Furthermore, the model allows us to calculate the probability of the velocity of a ganglion of any assigned size. The procedure may be useful for estimating the time required by the mobile fraction of a bank of oil to leave the porous bed.

The model has been developed for simulating the saturated zone of an aquifer. The range of particle diameters tested simulates sands from fine to coarse. The limitation of the model resides in the fact that regularly and uniformly shaped and sized particles have been considered.

Acknowledgements

This work was financed by “Dipartimento della Protezione Civile-Consiglio Nazionale delle Ricerche. Gruppo Nazionale per la Difesa dai Rischi Chimico Industriale Ecologici”.

References

[1] K.M. Ng, A.C. Payatakes, Stochastic simulation of the motion, breakup and stranding of oil ganglia in water-wet granular porous media during immiscible displacement, AIChE J. 26 (1980) 419–428.
[2] A.C. Payatakes, K.M. Ng, R.W. Flumerfelt, Oil ganglion dynamics during immiscible displacement: model formulation, AIChE J. 26 (1980) 430–443.
[3] M.M. Dias, A.C. Payatakes, Network models for two-phase flow in porous media, J. Fluid Mech. 164 (1986) 305–336.
[4] D.G. Avraam, A.C. Payatakes, Flow mechanisms, relative permeabilities, and coupling effects in steady-state two-phase flow through porous media. The case of strong wettability, Ind. Eng. Chem. Res. 38 (1999) 778–786.
[5] S.E. Powers, L.M. Abriola, W.J. Weber Jr., An experimental investigation of nonaqueous phase liquid dissolution in saturated subsurface systems: steady state mass transfer rates, Water Resource Res. 28 (1992) 2691–2705.
[6] A. Mayer, C. Miller, The influence of porous medium characteristics and measurement scale on pore-scale distribution of residual nonaqueous-phase liquids, J. Contamin. Hydrol. 11 (1992) 189–213.
[7] A.S. Mayer, C.T. Miller, An experimental investigation of pore-scale distribution of nonaqueous phase liquids at residual saturation, Transport in Porous Media 10 (1993) 57–80.
[8] K.D. Pennel, G.A. Pope, L.M. Abriola, Influence of viscous and buoyancy forces on the mobilization of residual tetrachloroethylene during surfactant flushing, Environ. Sci. Technol. 30 (1996) 1328–1335.
[9] R.B. Bird, W.E. Stewart, E.N. Lightfoot, Transport Phenomena, Wiley, NY, 1960, p. 200.
[10] G. Alfani, S. Andreutti, Indagine teorica e sperimentale sul meccanismo di mobilizzazione e frammentazione di oli inquinanti in mezzi porosi saturi, Tesi di Laurea in Ingegneria Chimica, Università di Napoli Federico II, 2002.
[11] R. Clift, J.R. Grace, M.E. Weber, Bubbles, Drops and Particles, Academy Press, NY, 1978, p. 33.